

Primordial Synthesis: \mathcal{F} - $SU(5)$ SUSY Multijets, 145-150 GeV LSP, Proton & Rare Decays, 125 GeV Higgs Boson, and WMAP7

Tianjun Li,^{1,2} James A. Maxin,² Dimitri V. Nanopoulos,^{2,3,4} and Joel W. Walker⁵

¹*State Key Laboratory of Theoretical Physics and Kavli Institute for Theoretical Physics China (KITPC), Institute of Theoretical Physics, Chinese Academy of Sciences, Beijing 100190, P. R. China*

²*George P. and Cynthia W. Mitchell Institute for Fundamental Physics and Astronomy, Texas A&M University, College Station, TX 77843, USA*

³*Astroparticle Physics Group, Houston Advanced Research Center (HARC), Mitchell Campus, Woodlands, TX 77381, USA*

⁴*Academy of Athens, Division of Natural Sciences, 28 Panepistimiou Avenue, Athens 10679, Greece*

⁵*Department of Physics, Sam Houston State University, Huntsville, TX 77341, USA*

We examine the first ATLAS Collaboration $\sqrt{s} = 8$ TeV 5.8 fb^{-1} supersymmetry (SUSY) multijet data observations in the context of No-Scale Flipped $SU(5)$ with extra TeV-Scale vector-like flippon multiplets, dubbed \mathcal{F} - $SU(5)$, finding that the recent 8 TeV collider data is statistically consistent with our prior 7 TeV results. Furthermore, we synthesize all currently ongoing experiments searching for beyond the Standard Model (BSM) physics with this fit to the 8 TeV data, establishing a suggestive global coherence within a No-Scale \mathcal{F} - $SU(5)$ high-energy framework. The SUSY mass scale consistent with all BSM data consists of the region of the \mathcal{F} - $SU(5)$ model space within $660 \lesssim M_{1/2} \lesssim 760$ GeV, which corresponds to sparticle masses of $133 \lesssim M(\tilde{\chi}_1^0) \lesssim 160$ GeV, $725 \lesssim M(\tilde{t}_1) \lesssim 845$ GeV, and $890 \lesssim M(\tilde{g}) \lesssim 1025$ GeV. We suggest that the tight non-trivial correspondence between the SUSY multijets, direct and indirect searches for dark matter, proton decay, rare-decay processes, the observed Higgs boson mass, and the measured dark matter relic density, is strongly indicative of a deeper fundamental relationship. We additionally suggest a simple mechanism for enhancing the capture efficiency of \mathcal{F} - $SU(5)$ SUSY multijets, which results in a 93% suppression in ATLAS reported background events, but only a 27% decrease in Monte Carlo simulated \mathcal{F} - $SU(5)$ multijet events.

PACS numbers: 11.10.Kk, 11.25.Mj, 11.25.-w, 12.60.Jv

I. INTRODUCTION

In this work we extend the projection of Monte Carlo (MC) collider-detector simulation from the No-Scale \mathcal{F} - $SU(5)$ model [1–21] onto data collected at the Large Hadron Collider (LHC) experiment into the emerging results for the 2012 $\sqrt{s} = 8$ TeV run [22, 23]. We undertake a broader survey of the component sources of error, both internal to our analysis and external, that may obscure a clear delineation of the experimentally favored \mathcal{F} - $SU(5)$ mass scale. Our primary finding is that, while the gaugino mass centrally indicated by the newer data is discernibly elevated relative to the lower energy 2011 run, the mutual overlap between the associated 2σ uncertainties remains sufficient to declare the results statistically consistent.

A perfectly direct comparison between the $\sqrt{s} = 7$ TeV [24, 25] and available $\sqrt{s} = 8$ TeV [22, 23] search strategies is complicated in one studied example [23] by modifications to the channel segregation and selection cuts that have presumably been employed for optimization of the expected cross section limits for certain simplified Supersymmetry (SUSY) models. In another case [22], we presently suggest an alternative selection cut threshold derived out of the finely grained bin-wise results supplied by the ATLAS collaboration that has the dual benefit of i) improving the statistical correlation between the published 2011 and 2012 results, and ii)

substantially further taxing the strength of the Standard Model (SM) background competition while assessing only a comparatively modest duty against the expected \mathcal{F} - $SU(5)$ signal. Simultaneously, we remain mindful of alternative factors that may yet play a role in the ultimate interpretation of contemporary circumstances, such as the difficulty in establishing supersymmetric cross sections at the Next to Leading Order (NLO) [26], and the possibility of an understandably cautious default institutional stance in the estimation of event backgrounds [27]. Moreover, although the relevant SUSY cross sections associated with collider operation at $\sqrt{s} = 8$ TeV may be a few-fold enhanced relative to those at $\sqrt{s} = 7$ TeV, the luminosities integrated in either case remain for now comparable, and it similarly remains somewhat unclear whether the onus of reconciliation between these observations will come to rest more so with an upward statistical fluctuation in the former season of data collection or a downward fluctuation in the latter.

We emphasize that our sympathy for the No-Scale \mathcal{F} - $SU(5)$ model derives not out of any single collider based result, but rather from an aggregation of successful comparisons to data on the Cold Dark Matter (CDM) relic density, the mass of the lightest Charge conjugation-Parity (CP) even Higgs field, post-SM contributions to rare processes, Astro-physical line-sources in the gamma-ray spectrum, and proton decay, coupled with deep structural motivations that include basic string- and F-theoretic model building consistency, the

reductionism and cosmological relevance of No-Scale Supergravity, and the full range of phenomenological advantages associated with the Flipped $SU(5)$ Grand Unified Theory (GUT). The specificity afforded by this tightly defined global framework is both the mechanism by which detailed comparison against the collider results is facilitated, and also an agent of intuition and context for the rationalization and interpretation of those results. This is not to our perception wishful, but rather a consciously guided logic corresponding to the net accumulation of prior probabilities in the Bayesian sense. It is indeed the inclusive primordial synthesis of diverse experimentation and well motivated theory.

II. THE \mathcal{F} - $SU(5)$ MODEL

Supersymmetry naturally solves the gauge hierarchy problem in the SM, and suggests (given R parity conservation) the lightest supersymmetric particle (LSP) as a suitable cold dark matter candidate. However, since we do not see mass degeneracy of the superpartners, SUSY must be broken around the TeV scale. In GUTs with gravity mediated supersymmetry breaking, called the supergravity models, we can fully characterize the supersymmetry breaking soft terms by four universal parameters (gaugino mass $M_{1/2}$, scalar mass M_0 , trilinear soft term A , and the low energy ratio of Higgs vacuum expectation values (VEVs) $\tan\beta$), plus the sign of the Higgs bilinear mass term μ .

No-Scale Supergravity was proposed [28] to address the cosmological flatness problem, as the subset of supergravity models which satisfy the following three constraints: i) the vacuum energy vanishes automatically due to the suitable Kähler potential, ii) at the minimum of the scalar potential there exist flat directions that leave the gravitino mass $M_{3/2}$ undetermined, iii) the quantity $\text{Str}\mathcal{M}^2$ is zero at the minimum. If the third condition were not true, large one-loop corrections would force $M_{3/2}$ to be either identically zero or of the Planck scale. A simple Kähler potential that satisfies the first two conditions is [28, 29]

$$K = -3\ln(T + \bar{T} - \sum_i \bar{\Phi}_i \Phi_i), \quad (1)$$

where T is a modulus field and Φ_i are matter fields. The third condition is model dependent and can always be satisfied in principle [30]. For the simple Kähler potential in Eq. (1) we automatically obtain the No-Scale boundary condition $M_0 = A = B_\mu = 0$ while $M_{1/2}$ is allowed, and indeed required for SUSY breaking. Because the minimum of the electroweak (EW) Higgs potential $(V_{EW})_{min}$ depends on $M_{3/2}$, the gravitino mass is determined by the equation $d(V_{EW})_{min}/dM_{3/2} = 0$. Thus, the supersymmetry breaking scale is determined dynamically. No-scale supergravity can be realized in the compactification of the weakly coupled heterotic string theory

[31] and the compactification of M-theory on S^1/Z_2 at the leading order [32].

In order to achieve true string-scale gauge coupling unification while avoiding the Landau pole problem, we supplement the the standard \mathcal{F} -lipped $SU(5) \times U(1)_X$ [33–36] SUSY field content with the following TeV-scale vector-like multiplets (flippons) [37]

$$\left(XF_{(\mathbf{10},\mathbf{1})} \equiv (XQ, XD^c, XN^c), \overline{XF}_{(\overline{\mathbf{10}},-\mathbf{1})} \right), \\ (Xl_{(\mathbf{1},-\mathbf{5})}, \overline{Xl}_{(\mathbf{1},\mathbf{5})} \equiv XE^c), \quad (2)$$

where XQ , XD^c , XE^c , XN^c have the same quantum numbers as the quark doublet, the right-handed down-type quark, charged lepton, and neutrino, respectively. Such kind of models can be realized in \mathcal{F} -free \mathcal{F} -hermionic string constructions [38], and \mathcal{F} -theory model building. Thus, they have been dubbed \mathcal{F} - $SU(5)$ [39].

III. THE ROLE OF MODEL-SPECIFIC PREDICTIONS

Significant particle physics searches of the past few decades had the benefit of a well developed Standard Model framework, leading to reliable theoretically based predictions and expectations. By contrast, the view available for steering the ongoing SUSY search is rather more clouded, with the symmetry breaking mechanism, the boundary conditions and level of universality inter-relating high-energy model parameters, and even the reality of low-energy SUSY itself still unknown. The LHC SUSY search effort is at the present, relatively speaking, in its very early stages. While the collaborations must understandably prefer a model-agnostic point of view, and insist on a much larger accumulation of data before a possible presence of beyond the Standard Model (BSM) physics is acknowledged, our role as a small theory group is distinct, yet complementary. Crucially, we have the unique freedom to focus not on the general, but rather the specific. Nature, after all, is the physical embodiment of but one single framework, possessed of features that may be cloaked to the parallel consideration of all conceivable morphologies. Given the rapid encroachment upon the leading BSM candidates' model spaces that has been observed during the first phase of LHC operation [40], the likelihood that alternatively viable conceptions such as No-Scale \mathcal{F} - $SU(5)$ may now drive the discussion has become sharply heightened. In particular, the specificity of such a context may both facilitate the global interpretation of experimental results and suggest preferred tactics for future searches.

A central question facing any attempt to compare a specific SUSY model construction against the emerging LHC data is that of how to correctly interpret mass limits published by the collaborations that are derived under the assumption of a highly simplified particle content or an alternatively conjectured theoretical SUSY

framework, typically of the CMSSM or mSUGRA variety. Such examples often decouple all SUSY fields other than the neutralino and gluino octet, or otherwise impose strict mass degeneracies, and may unrealistically force key branching ratios to unity. Our reading of limits of this type is that their merit is largely as a standardized metric for quantifying the overall “strength” of the search relative to prior surveys, whereas the applicability to any given physical scenario is somewhat less direct, and highly model dependent. In particular, it is well known that breaking the squark mass degeneracy into a strongly differentiated hierarchy may result in the substantial production of low transverse momentum jets that can evade currently favored thresholds for reconstruction. As such, we caution against an overly literal application of the mass limits established via these surveys to the \mathcal{F} - $SU(5)$ context. Moreover, we suggest that studies such as our own may fill a vital gap of information by providing independent data-driven demarcation of mass limits specifically applicable to certain realistic models, inclusive of all applicable sources of uncertainty.

The adoption of an exclusively specified analysis framework also affords some additional measure of resolution in the attempt to associate collider results from individual search channels with the signature production modes of the model under study. Apparently isolated details that might be overlooked in a model-independent approach may be granted additional significance within the context of a unifying model that allows for their mutual correlation. In conjunction, a decoupling of the corporate inertia associated with the need to assimilate multiple incompatible perspectives allows for a more lithe response to the volatile environment of a rapidly accumulating data store. Having said that, our job is not to replace, nor even to reproduce, the ATLAS experimental SUSY search analyses of Refs. [22, 23]. Rather, our focus is simply to assemble clues relevant to determination of the fate of one particular highly realistic model that might escape comment within a more diluted scope. Whereas ATLAS and CMS might bet on black or on red, we shall bet on green. The odds are certainly longer, but the payout may be commensurately greater.

IV. 8 TEV SUSY MULTIJETS

The No-Scale \mathcal{F} - $SU(5)$ model leverages the β -function coefficient b_i modifications induced by inclusion of the vector-like flippon multiplets to flatten the $SU(3)$ Renormalization Group Equation (RGE) running ($b_3 = 0$) [1], generating a characteristic mass texture of $M(\tilde{t}_1) < M(\tilde{g}) < M(\tilde{q})$, featuring a light stop and gluino that are lighter than all other squarks. This distinctive hierarchy is highly stable across the full viable parameter space, and is rescaled *en masse* according to action of the isolated dimensionful parameter $M_{1/2}$. We are not aware of any CMSSM/mSUGRA constructions in which this mass ordering is precisely replicated. The small light stop and

gluino mass splitting is generated by the same strongness of the Higgs to top quark couplings that provide the essential lifting of the MSSM Higgs boson mass. A direct consequence of this spectrum is a distinctive event topology beginning with the pair-production of squarks \tilde{q} and/or gluinos \tilde{g} in the initial hard scattering process, where each squark will most likely produce gluinos via $\tilde{q} \rightarrow q\tilde{g}$. Gluinos will then likely decay either through light stops by $\tilde{g} \rightarrow \tilde{t}_1\bar{t} \rightarrow t\bar{t}\tilde{\chi}_1^0$, or through $\tilde{g} \rightarrow q\bar{q}\tilde{\chi}_1^0$, with each gluino producing 2–6 jets. Therefore, the gluino-mediated stop channel diagram, which is most probable in \mathcal{F} - $SU(5)$, can produce up to 12 jets from a single pair-production gluino event [5, 6].

The unique rescaling of the No-Scale \mathcal{F} - $SU(5)$ SUSY particle hierarchy with respect to variation of $M_{1/2}$ implies a progressive widening of the mass-gap separating the gluino and light stop that yields a very interesting threshold transition. Specifically, the production of light stops in the previously described gluino-mediated channel abruptly shifts from off-shell to on-shell at $M_{1/2} = 729$ GeV, where $M(\tilde{g}) - M(\tilde{t}_1) = M(t)$. This effect will produce non-ignorable consequences for certain collider signatures, driven by the fact that $\tilde{g} \rightarrow \tilde{t}_1\bar{t}$ occurs at a 100% branching fraction for $M_{1/2} > 729$ GeV, effectively suppressing $\tilde{g} \rightarrow q\bar{q}\tilde{\chi}_1^0$. We shall examine this transition with care here and account for its effect in our results.

We have previously extensively studied [14, 16–18] the ATLAS and CMS 1, 2, and 5 fb^{-1} LHC data observations in the context of \mathcal{F} - $SU(5)$. Small, but curious, excesses beyond the Standard Model expectations were observed in the initial 1–2 fb^{-1} of multijet data at $\sqrt{s} = 7$ TeV [41–43], which we demonstrated could be neatly and globally explained as supersymmetry production [11, 14, 16] within the No-Scale \mathcal{F} - $SU(5)$ model. Assuming a purely authentic signal, we projected the anticipated growth forward to 5 fb^{-1} at 7 TeV. Upon subsequent release of the corresponding 5 fb^{-1} experimental results, we found these projections to be well substantiated in the data superser [17, 18], with a consistently isolated SUSY mass scale and a commensurate signal intensification. We interpreted this finding as an amplification of the likelihood that the small observed excesses were indeed largely attributable to fundamental physics, and not random background statistical fluctuation.

Completion of the first $\sqrt{s} = 8$ TeV SUSY multijet searches by ATLAS [22, 23] compels extension of the comparative \mathcal{F} - $SU(5)$ analysis undertaken at 7 TeV [14, 16–18] into the elevated beam collision energy context. Our effort is somewhat complicated at the outset by irreversible alterations to the 4-jet, 5-jet, and 6-jet SUSY search strategies of Ref. [23] from the previous 7 TeV partitions [24]. In the case of those SUSY searches adhering to a ≥ 7 , ≥ 8 , and ≥ 9 cut on jets [22], we observe that a more accommodative cut for discovery of \mathcal{F} - $SU(5)$ can be implemented by raising the ATLAS imposed $E_T^{\text{Miss}}/\sqrt{H_T} > 4$ $\text{GeV}^{1/2}$ requirement to a harder > 8 $\text{GeV}^{1/2}$. Averaged across all published search

channels at both 7 and 8 TeV, this escalation further reduces the already severely truncated SM background component extracted from the graphical bin-by-bin ATLAS analysis by a full 93%, while preserving a strong majority of critical \mathcal{F} - $SU(5)$ SUSY events, which experience only a 27% reduction in our Monte Carlo simulation. Such drastic increases in efficiency being rather hard to come by, this simple modification is one that we heartily recommend for further investigation to our experimental colleagues at the LHC collaborations. Moreover, we find that the residually observed signal proportion scales much more linearly between the 7 and 8 TeV results with this modification than without. In fact, the suggested lifting of the minimum boundary on the observable ratio $E_T^{\text{Miss}}/\sqrt{H_T}$ has existing precedent at ATLAS in Ref. [44], where a threshold of 11 GeV^{1/2} was imposed. Curiously, a simple visual inspection of Figure (5) in Ref. [44] also clearly indicates that a hard cut of $E_T^{\text{Miss}}/\sqrt{H_T} > 11$ GeV^{1/2} implies all surviving signal excesses in this SUSY light stop search must emanate from events with 9–10 jets. Event production in this ultra-high jet multiplicity regime is the leading collider signature of \mathcal{F} - $SU(5)$, wholly in concordance with our originally suggested search prescription [5, 6], providing ample justification for a more harsh and efficient cut on $E_T^{\text{Miss}}/\sqrt{H_T}$, as we shall apply in our work here.

To most effectively portray \mathcal{F} - $SU(5)$ against the circumstance of the rather light data accumulation to date, we take a cue from the recent LHC Higgs boson search, where of the five expected production channels, only the $\gamma\gamma$ and ZZ channels were initially productive in 2011, and thus utilized for compelling evidence of Higgs boson production. In tandem, the $\tau\tau$, WW , and $b\bar{b}$ channels either displayed under-production or no evidence at all, though these unproductive channels did not sway the convincing argument in December 2011 that indeed the Higgs boson was on the verge of eclipsing a significant observational threshold. We believe that an extension of this search tactic is suitable to our current purpose, and thus elect to partition the available data channels into two categories: i) inclusive, representing those productive searches demonstrating some activity over and above the expectations for the SM background, and ii) exclusive, denoting those searches embodying a null set of events beyond expectations. Within the inclusive data set, we search for correlations in the form of a consistently isolated \mathcal{F} - $SU(5)$ mass scale associable with each observed excess. For the exclusive data sets, we verify overlap of the suggested lower bound on $M_{1/2}$ with the value favored by the former best fit. We utilize the signal significance metric $S = 2 \times (\sqrt{N_S + N_B} - \sqrt{N_B})$ to enact the described partition, selecting those multijet searches from Refs. [22, 23] that exceed a specified minimum level of significance. For our study here, we elect a lower limit of $S = 2 \times (\sqrt{N_S + N_B} - \sqrt{N_B}) \geq 1$.

We find that only five of the seventeen multijet searches satisfy the $S = 2 \times (\sqrt{N_S + N_B} - \sqrt{N_B}) \geq 1$ condition: 7j80, 8j55, and 8j80 of Ref. [22], in conjunction with

SRE Loose and SRE Medium of Ref. [23]. The 7j80 requires a minimum of 7 jets and jet $p_T > 80$ GeV, while 8j55 applies a cut at ≥ 8 jets and $p_T > 55$ GeV, with 8j80 also requiring at least 8 jets with $p_T > 80$ GeV. The SRE Loose and SRE Tight both retain only those events with 6 jets and $p_T > 60$ GeV, though the Loose prescription sets a cut on effective mass, defined to be the scalar sum of the transverse momenta of the leading N jets together with E_T^{Miss} , at $M_{\text{eff}} > 1$ TeV and $E_T^{\text{Miss}}/M_{\text{eff}} > 0.3$, whereas the Medium case applies the cut at $M_{\text{eff}} > 1.3$ TeV and $E_T^{\text{Miss}}/M_{\text{eff}} > 0.25$. Although we would like to see a somewhat lower threshold on the reconstructed jet transverse momentum, and have advocated a value as low as $p_T \gtrsim 20$ GeV in Refs. [5, 6], we acknowledge the technical hurdles which make such an extension difficult. However, this practical limitation does leave a large region of the SUSY parameter space unexplored, to which the commonly promoted simplified SUSY mass exclusion diagrams may be quite sensitive. We tender for comparison the case of the ATLAS light stop search in Ref. [44], which seemingly successfully realized a soft p_T cut on jets of $p_T > 25$ GeV, obtaining in the process crucial information on excess production in events with 9–10 jets.

The salvaging of these five strategies from the full ATLAS SUSY multijet 8 TeV search campaign affords us with five degrees of freedom (DOF) with which to construct a multi-axis χ^2 fitting procedure. However, these five DOF are not all statistically independent, supplying us with an effective DOF count which is somewhat less than five. While we presently forgo a detailed weighting and recombination procedure, we have explicitly verified that a reduction to three effective DOF's only marginally collapses the width of the χ^2 error margins, corresponding specifically to an elevation of the 2σ lower SUSY mass limit intersection by about 10 GeV. Additionally, we have generically quantified the correlated overlap existing between Monte Carlo events surviving each considered search strategy, according to the prescription $N_{\text{Common}}/\sqrt{N_A \times N_B}$. This statistic is reported in Table I for each pairing of channels A and B, where N_{Common} is the count of overlapping events, and N_A , N_B are the counts of events passing each selection individually. We observe a modest correlation averaging about $\sim 50\%$ amongst only the ≥ 7 -jet, ≥ 8 -jet, and ≥ 9 -jet multijet searches internal to Ref. [22], compared to a very small overlap of the ≥ 7 -jet, ≥ 8 -jet, and ≥ 9 -jet searches with the 6-jet searches of Ref. [23]. Likewise, the SRE Loose and SRE Medium exhibit a very high correlation, in line with expectations.

The No-Scale \mathcal{F} - $SU(5)$ experimentally viable parameter space features a distinctive abrupt transition from off-shell light stop production to on-shell. We have noted this trait in prior work [16, 17], though we had not previously explicitly taken this interesting aspect into account in our SUSY mass fittings. We shall ascertain the entire consequence of this sharp transition in this work, the effect of which we determine to be non-negligible. We further attempt to integrate a more realistic compilation

TABLE I: Values of Correlation Function measuring statistical independence amongst all SUSY searches satisfying the condition $2 \times (\sqrt{N_S + N_B} - \sqrt{N_B}) \geq 1$. A higher value indicates a higher overlap of events between the two searches, where the Correlation Function can assume percentage values from 0 to 100.

	8j55	8j80	SREL	SREM
7j80	58.7	55.5	15.0	24.5
8j55	–	43.1	23.2	32.8
8j80	–	–	7.1	12.7
SREL	–	–	–	68.6

of all the experimental and theoretical uncertainties into our analysis, a comprehensive treatment appended to our more abridged policy toward accumulated uncertainties in past work. The mentioned uncertainty may arise from many sources, the most obvious being the Poisson statistical fluctuations of the reported event counts, the official collaboration estimates of the SM background error, and imperfections in our own Monte Carlo event generation, detector simulation, and event selection processing phase. For instance, the typical margin of error on the PGS4 [45] detector simulation we utilize is quoted at 20%, with the caveat that circumstances may sometimes conspire to produce a factor as large as two. There are also more subtle potential sources, both internal and external, of systematic uncertainty such as i) limitations on computational accuracy of the flippon-modified \mathcal{F} - $SU(5)$ SUSY spectrum and Higgs boson mass, and 2) the possibility that the NLO QCD corrections to multi-jet production cross sections could be somewhat smaller than, perhaps even only 60% of, the Collaboration estimates [26], as applied to the simulation of both the supersymmetry and SM background event production rate. This latter effect would result in an overestimation of background levels and over-production of SUSY events in the popular Monte-Carlo codes, potentially masking the observation of legitimate experimental SUSY signatures, while simultaneously falsely escalating the SUSY mass scale required for sufficient event suppression. This could also account for the suggestion of an apparent bias toward large p-values in the global analysis of early LHC results [27]. Our approach for addressing these difficulties in the present work is two-fold. Firstly, we undertake the described quantification of the chi-square deviation separating the experimental results from the \mathcal{F} - $SU(5)$ collider-detector simulation for a continuous string of $M_{1/2}$ values spanning the otherwise viable model space. Secondly, we repeat this analysis while enhancing or suppressing the nominal Monte Carlo event count by a selected overall rescaling factor, adopting the outer convolution of the mass boundaries as limits on the model.

The consequence of compounded uncertainties on the SUSY mass spectrum in our \mathcal{F} - $SU(5)$ computations is depicted in Figure (1) for the selected search case of 7j80. Shown are the nominal number of surviving events after

all data cuts, and also the relative increase and decrease by factors of two and four. Rescaling by a factor as large as four might be interpreted as a worst-case scenario, although we deem the more modest factor of two to be quite reasonably necessary. The data lines in Figure (1) represent linear fittings to a specified set of benchmarks, the characteristics of which shall be elaborated upon in the next section. Graphically displayed is the off-shell to on-shell transition, an aspect alone that reduces the observed cross section for $M_{1/2} > 729$ GeV by nearly a factor of two for the case of 7j80. For 7j80, we see that the best fit to the nominal number of excess events above the background expectations reported by ATLAS is $M_{1/2} = 756$ GeV, with a BSM 2σ upper limit falling at $M_{1/2} \geq 700$ GeV. On the other hand, adjustments upward and downward by the fixed multiples of two and four translate the BSM 2σ upper limit to $M_{1/2} \geq 700_{-235}^{+100}$ GeV, represented by the yellow region in Figure (1), permitting the majority of the \mathcal{F} - $SU(5)$ viable parameter space to remain experimentally plausible. This corresponds to sparticle masses of $M(\tilde{\chi}_1^0) \geq 142_{-55}^{+25}$ GeV, $M(\tilde{t}_1) \geq 775_{-281}^{+114}$ GeV, and $M(\tilde{g}) \geq 944_{-309}^{+134}$ GeV (see bottom scales in the ‘‘Primordial Synthesis’’ Figure (3) for $M_{1/2}$ to gluino and light stop mass conversions).

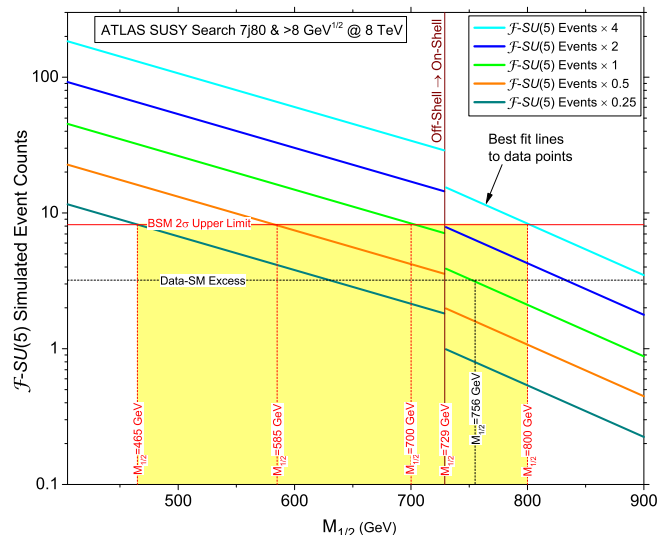


FIG. 1: Measure of uncertainty in the complete sequence of SUSY mass spectrum calculations through the detector simulations in No-Scale \mathcal{F} - $SU(5)$ for the 7j80 SUSY multijets search using the optimized cut of $E_T^{\text{Miss}}/\sqrt{H_T} > 8 \text{ GeV}^{1/2}$. We increase and decrease the nominal number of \mathcal{F} - $SU(5)$ events surviving all the ATLAS prescribed cuts by factors of two and four to ascertain the effect of accumulated uncertainties on the best fit SUSY mass scale. We show the 2σ BSM upper limit on the number of collider events for each multiple of the nominal number of events. The yellow region illustrates the total uncertainty on the 2σ BSM upper limit when taking into account all experimental and theoretical uncertainties.

The completion of a multi-axis χ^2 analysis is facilitated by execution on twenty-one benchmark samples an

in-depth Monte Carlo collider-detector simulation of all 2-body SUSY processes based on the `MadGraph` [46, 47] program suite, including the `MadEvent` [48], `PYTHIA` [49] and `PGS4` chain. The SUSY particle masses are calculated with `MicrOMEGAs 2.4` [50], applying a proprietary modification of the `SuSpect 2.34` [51] codebase to run the flippon-enhanced RGEs. We implement a modified version of the default ATLAS detector specification card provided with `PGS4` that calls an anti-kt jet clustering algorithm, indicating an angular scale parameter of $\Delta R = 0.4$. The resultant event files are filtered according to a precise replication of the selection cuts specified by the ATLAS Collaboration in Refs. [22, 23], employing the script `CutLHCO 2.0` [52] to implement the post-processing cuts.

Our χ^2 analysis of the initial $\sqrt{s} = 8$ TeV ATLAS multijet searches [22, 23] is depicted in the two panels of Figure (2), first for the five inclusive search strategies with signal significance $2 \times (\sqrt{N_S + N_B} - \sqrt{N_B}) \geq 1$ and next for the thirteen channels showing no corresponding visible excess above the SM background. The Cumulative Distribution Function (CDF) percentage labeled on the right-hand axis of each plot is a statistical tool that establishes the fraction of trials (for a fixed number of statistically independent variables) where Gaussian fluctuation of each of variable will yield a net deviation from the null hypothesis that is not larger than the corresponding χ^2 value referenced on the left-hand axis. The distinction between a one-sided and two-sided limit is made with regards to the placement of the 0, 1, 2- σ bounds relative to the numerical value of the CDF. A two-sided limit, as adopted in the initial panel for the χ^2 best-fit minimization against $M_{1/2}$ using searches with visible excesses, is appropriate when meaningful deviations may be anticipated in either direction away from the median. Particularly small χ^2 values imply a better fit to the data by the assumed signal (at a certain confidence level) than what could be attributed to random fluctuations around the SM, while excessively large χ^2 values disfavor a given $M_{1/2}$ relative to the SM-only null hypothesis. In this case, the usual 1 and 2- σ 68% and 95% consistency integrations enclose areas symmetrically distributed about the mean, such that centrally inclusive boundary lines are drawn at the CDF percentages 2.2%, 15.9%, 84.1%, and 97.7%. It should be noted that this method implicitly assumes the displayed channels to be statistically uncorrelated, which is not perfectly applicable in the current case. A compensating reduction in the effective degrees of freedom from the nominal value of three would have the effect of marginally lowering the quoted CDF scale values relative to the left-hand χ^2 axis, slightly compressing the displayed error margins.

In the analysis presented in the second panel, we are instead intent on establishing a global lower bound on $M_{1/2}$ by consideration of those studies without compelling hints of new physics. The one-sided limit employed here is appropriate when the null hypothesis is disfavored only for deviations in a single direction, in

this case toward excessively large χ^2 values. The full exclusion is thus shifted toward a single tail of the distribution, and the exclusion bounds are drawn directly at CDF values of 68% and 95%. Although matching bounds beneath the median are also plotted for visual reference, they are less meaningful in this context. To cope with the expected strong signal inter-dependence in this case, and to avoid disproportionately emphasizing or suppressing the influence of either of the two broad search strategies, we have opted to average the χ^2 deviation at each $M_{1/2}$ across each closely related channel. The results are then presented as a χ^2 analysis in two effective or composite “unit strength” degrees of freedom.

The searches demonstrating an excess allow for the isolation of a best fit to the rate of \mathcal{F} - $SU(5)$ SUSY production, as regulated by the mass parameter $M_{1/2}$. The five minima (which again hail from two broadly independent search strategies, as analyzed in Table I) are in excellent agreement, falling within the range of 756 GeV to 796 GeV. The overall best fit for productive channels is at 792 GeV, and the intersections below and above with the median Cumulative Distribution Function (CDF) probability span a range of about 730 GeV to 990 GeV. This upper bound is already beyond the range of $M_{1/2}$ values around 900 GeV at which the \mathcal{F} - $SU(5)$ LSP becomes charged [7], generating a well-defined finite truncation of the viable model search space. The 2σ χ^2 intersection for the inclusive searches sets a lower bound around 710 GeV. The 2σ exclusion range from the non-productive channels is near 735 GeV in the second panel. The depth of the χ^2 well is rather remarkable, with the SM limit rising well above the median probability, even without compensation for the reduction in effective degrees of freedom.

It is clear that this first round of data analyzed at the elevated collision energy does seem to systematically isolate a somewhat heavier spectrum than that suggested by the corresponding $\sqrt{s} = 7$ TeV [24, 25] data, previously analyzed in Refs. [17, 18, 20, 21]. This is identical to the statement that growth of signal relative to background is comparatively suppressed in the higher energy results, and that the most optimistic expectations for a linear extrapolation of the prior ratios have not in full materialized. For comparison, a structurally similar study of the earlier LHC run [18] isolated a best fit for $M_{1/2}$ at 658 GeV, with the median intersection stretching from 600 GeV to 770 GeV. However, including the previously described error analysis, our parallel χ^2 treatment of down-scaled ($\times 1/2$) event production (not pictured) suggests a range for the intersection with the probability median of the inclusive searches that extends from about 660 GeV to 930 GeV. The 2σ intersections for the inclusive and exclusive searches drop to approximately 620 GeV and 660 GeV, respectively. We thus conservatively establish a lower bound for the \mathcal{F} - $SU(5)$ gaugino mass of about $M_{1/2} \geq 660$ GeV, corresponding to LSP, gluino and light stop masses of approximately 133 GeV, 890 GeV, and 725 GeV, respectively. The 1/4 strength

event down-scaling, which we judge to be a rather more extreme scenario, generates a best fit at 651 GeV, intersections with the median CDF value around 560 GeV and 870 GeV, and intersections with the 2σ line around 515 GeV and 560 GeV for the inclusive and exclusive searches, respectively.

Our survey of the $\sqrt{s} = 8$ TeV results thus suggest that the benchmark favored in the current report remains marginally consistent with that isolated by the $\sqrt{s} = 7$ TeV data. This statement is justified by the existence of a satisfactory mutual overlap between the masses encapsulated by the median 50% CDF intersections of the two studies, without resorting to any event rescaling. Moreover, the overall lower boundary extracted from the 8 TeV data at a down-scaling of 1/2 is essentially identical to the nominally established best fit at 7 TeV. The vital importance of individual model-specific comparisons to data is emphasized by a comparison of our derived $\tilde{\chi}_1^0$, \tilde{t}_1 , and \tilde{g} \mathcal{F} - $SU(5)$ mass limits with those established under simplified SUSY model assumptions by the ATLAS collaboration. The observed disparity suggests to us that the simplified limits may indeed exaggerate the bounds ascribable to physically realistic models, particularly with regards to the gluino mass, and that care should be exercised against their overly literal interpretation.

If indeed the reported excess production above the background estimates is the result of new physics and not attributed to background fluctuations, then the signal growth for larger statistics should remain roughly proportional to the increase in luminosity. We project the future signal significance in Table II and Table III of the five 8 TeV ATLAS 5.8 fb^{-1} searches exceeding the requirement $S = 2 \times (\sqrt{N_S + N_B} - \sqrt{N_B}) \geq 1$. We choose the milestone luminosities 10 fb^{-1} , 15 fb^{-1} , and 20 fb^{-1} , all reachable in 2012. Our method of projecting forward the ATLAS background, while serving our limited scope here adequately, can only be as reliable as the expectation of statistical, dynamic and procedural stability across the transition in luminosity and model. We also presume static ATLAS data cutting strategies in Refs. [22, 23] from 5.8 fb^{-1} to 20 fb^{-1} . The projections in Table II and Table III could be regarded as conservative, if we take into account the sizeable downward fluctuation already witnessed in the data observations from 7 TeV to 8 TeV, and we certainly do not consider an upside surprise in the signal significance going forward to be improbable. For example, the ATLAS 7 TeV background for SUSY search 7j80 increased by a factor of 6.6 from 1 fb^{-1} [42] to 4.7 fb^{-1} [25], and concurrently, the data observations increased by a factor of 5.0, displaying reasonable consistency with the growth in luminosity. By contrast, the ATLAS background increases by a factor of 3.3 from 5 fb^{-1} at 7 TeV to 5.8 fb^{-1} at 8 TeV, the same factor by which \mathcal{F} - $SU(5)$ 7j80 event counts increase in our simulations, but the data observations only increase by a factor of 1.7 [22]. Hence, the rate of change of the data observations from 1 fb^{-1} at 7 TeV to 5.8 fb^{-1} at 8

TeV has been markedly diminished with respect to the corresponding rate of change of the background and luminosity over this same period.

Although higher energy collider operation does induce larger SUSY cross sections and additional phase space headroom, the collected luminosity at 7 and 8 TeV still remains comparable. It remains to be seen whether these small discrepancies shall ultimately be attributed to primarily statistical or systematic origins in either or both of the independently collected data sets. Accordingly, we await the LHC data forthcoming through the conclusion of 2012 that could clarify whether this dichotomy is triggered by a downward fluctuation in the observed 8 TeV 5.8 fb^{-1} data or an upward fluctuation in the 7 TeV observed data, possibly also convoluted with either an overestimated background for 8 TeV or an underestimated background for 7 TeV.

TABLE II: Projected signal significance using the metric $S = 2 \times (\sqrt{N_S + N_B} - \sqrt{N_B})$ for 10 fb^{-1} , 15 fb^{-1} , and 20 fb^{-1} at $\sqrt{s} = 8$ TeV for the searches of Ref. [22] that surpass the condition $S = 2 \times (\sqrt{N_S + N_B} - \sqrt{N_B}) \geq 1$ for 5.8 fb^{-1} at 8 TeV, where N_s is the number of signal events and N_b is the number of background events.

fb^{-1}	7j80			8j55			8j80		
	N_s	N_b	S	N_s	N_b	S	N_s	N_b	S
10	5.5	3.1	2.3	6.1	5.9	2.1	1.5	0.2	1.8
15	8.3	4.6	2.9	9.2	8.9	2.6	2.4	0.2	2.3
20	11.0	6.2	3.3	12.3	11.8	2.9	3.1	0.3	2.6

TABLE III: Projected signal significance for the searches of Ref. [23] that surpass the condition $S \geq 1$ for 5.8 fb^{-1} at 8 TeV.

fb^{-1}	SRE Loose			SRE Medium		
	N_s	N_b	S	N_s	N_b	S
10	5.7	9.8	1.6	6.0	6.0	2.0
15	8.6	14.7	2.0	9.0	9.0	2.5
20	11.3	19.7	2.3	12.0	12.0	2.9

V. PRIMORDIAL SYNTHESIS

We previously advertised a conspicuously correlated region of the \mathcal{F} - $SU(5)$ model space adherent to experimentally derived constraints imposed upon the set of rare-decay processes consisting of the flavor changing neutral current processes $b \rightarrow s\gamma$ and $B_S^0 \rightarrow \mu^+\mu^-$, and the anomalous magnetic moment $(g-2)_\mu$ of the muon, the intersection of which we labeled as the *Golden Strip*. The recent calculation of the complete tenth-order QED terms for $(g-2)_\mu$ [53] has motivated a fresh inspection of these processes, expanding our original exploration for even deeper correlative behavior within a wider scope of

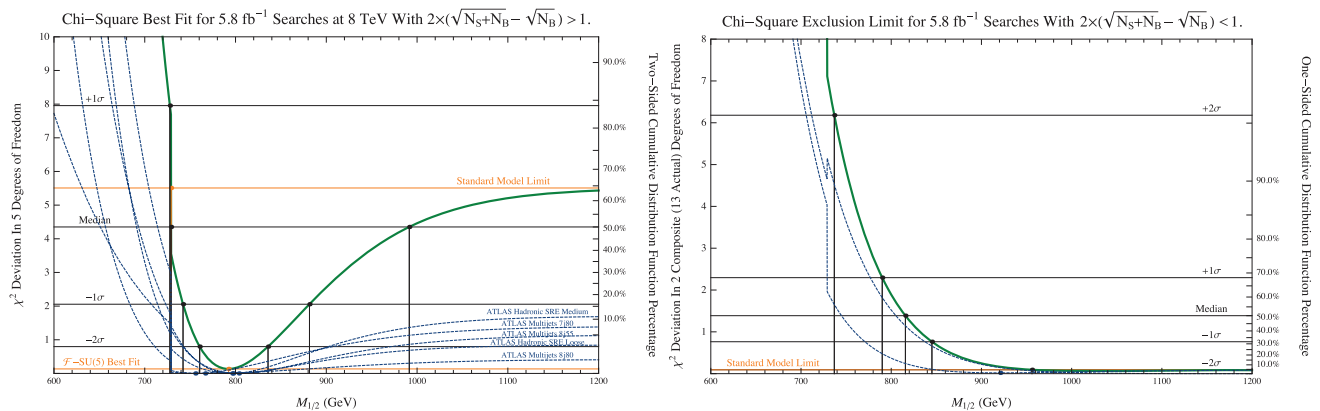


FIG. 2: We depict the χ^2 analyses of the 8 TeV ATLAS 5.8 fb^{-1} 7j80, 8j55, 8j80, SRE Loose, and SRE Medium Multijet search strategies from Refs. [22, 23] that exhibit a signal significance of $2 \times (\sqrt{N_S + N_B} - \sqrt{N_B}) \geq 1$ (left-hand pane), and the corresponding null searches of Refs. [22, 23] with $2 \times (\sqrt{N_S + N_B} - \sqrt{N_B}) < 1$ (right-hand pane). The thin dotted blue lines correspond to the individual χ^2 curves for each event selection for only the case of the nominal number of $\mathcal{F}\text{-}SU(5)$ events, which are summed into the thick green cumulative multi-axis χ^2 curves. The large discontinuity shown represents the transition from off-shell to on-shell light stop production at $M_{1/2} = 729 \text{ GeV}$.

experiments presently searching for supersymmetry and both direct and indirect evidence for dark matter. The natural synthesis of all these elements in an $\mathcal{F}\text{-}SU(5)$ framework exhibits clear global coherence.

The base of our investigation centers on the region of No-Scale $\mathcal{F}\text{-}SU(5)$ model space satisfying a set of stable bare-minimal experimental constraints [7], defined by consistency with the world-average top quark mass $172.2 \leq m_t \leq 174.4 \text{ GeV}$ [54], No-Scale boundary conditions $m_0 = A_0 = B_\mu = 0$, radiative electroweak symmetry breaking (EWSB), centrally observed 7-year WMAP cold dark matter density limits $0.1088 \leq \Omega h^2 \leq 0.1158$ [55], and LEP constraints on the lightest CP-even Higgs boson, light SUSY chargino, and neutralino masses. The union of all these bare-minimal constraints alone is certainly non-trivial, in particular the convergence of the No-Scale boundary conditions, most notably the requirement of vanishing B_μ , with the precision empirically measured 1σ uncertainties on the top quark mass m_t and relic density Ωh^2 .

The LHC observations of an $m_h \sim 125 \text{ GeV}$ light Higgs boson [56–58], while celebrated as a significant milestone in experimental particle physics, unexpectedly injected considerable turmoil into the landscape of supersymmetric models. Whereas the MSSM contribution to the Higgs boson mass is woefully insufficient to attain 125 GeV and concurrently generate a plausibly light and testable SUSY mass content at the 8 TeV LHC (simultaneously avoiding the invocation of fine-tuning to once again escape the gauge-hierarchy problem) the very favorable (and possibly necessary) contributions to the Higgs boson mass quite naturally supplied by the additional vector-like flippon multiplets provide the desired boost in $\mathcal{F}\text{-}SU(5)$ to produce an $m_h \sim 125 \text{ GeV}$ light Higgs boson. We have previously completed robust analyses of an $m_h \sim 125 \text{ GeV}$ Higgs boson in $\mathcal{F}\text{-}SU(5)$ [15, 21], demar-

cating a narrowly contoured strip carved out of the larger region formed by the application of the bare-minimal constraints. This strip of model space, clearly delineated in Refs. [19–21], comprises the intersection of an $m_h \sim 125 \text{ GeV}$ Higgs boson, 1σ variance on the WMAP 7-year relic density measurements and world-average top quark mass, and adherence to the No-Scale high-energy boundary conditions, the totality of which we shall heretofore refer to as the *125 GeV Higgs Strip*. Though the simple existence of such a strip is itself already noteworthy, a true model of nature must further exhibit profound correlation between *all* observable quantities, evident within the empirical uncertainties to which measurements obtained from current state-of-the-art technology is bound.

We now seek to synthesize the 125 GeV Higgs Strip with the amalgamation of complementary supersymmetry experiments, including our 8 TeV conclusions of the prior section. We begin with the original components of our Golden Strip [2, 7, 12], which are the key rare process limits on $Br(b \rightarrow s\gamma)$, $Br(B_S^0 \rightarrow \mu^+\mu^-)$, and Δa_μ on $(g-2)_\mu$ of the muon. For $b \rightarrow s\gamma$, we use the latest world average of the Heavy Flavor Averaging Group (HFAG), BABAR, Belle, and CLEO, which is $(3.55 \pm 0.24_{\text{exp}} \pm 0.09_{\text{model}}) \times 10^{-4}$ [59]. An alternate approach to the average [60] yields a slightly smaller central value, but also a lower error, suggesting $Br(b \rightarrow s\gamma) = (3.50 \pm 0.14_{\text{exp}} \pm 0.10_{\text{model}}) \times 10^{-4}$. See Ref. [61] for recent discussion and analysis. The theoretical SM contribution at the next-to-next-to-leading order (NNLO) is estimated at $Br(b \rightarrow s\gamma) = (3.15 \pm 0.23) \times 10^{-4}$ [62] and $Br(b \rightarrow s\gamma) = (2.98 \pm 0.26) \times 10^{-4}$ [63]. The addition of these errors in quadrature provides the 2σ limits of $2.86 \times 10^{-4} \leq Br(b \rightarrow s\gamma) \leq 4.24 \times 10^{-4}$. The recent precision improved LHCb constraints on the B-decay process $B_S^0 \rightarrow \mu^+\mu^-$ of $Br(B_S^0 \rightarrow \mu^+\mu^-) < 4.5(3.8) \times 10^{-9}$ at the 95% (90%) confidence level [64] are employed

here, though we find the entire viable \mathcal{F} - $SU(5)$ parameter space lies comfortably below this upper limit [19]. The new calculations of the tenth-order QED terms for the theoretical prediction of $(g-2)_\mu$ engenders a favorable shift in Δa_μ in the context of \mathcal{F} - $SU(5)$, where we apply the 2σ uncertainty of $6.6 \times 10^{-10} \leq \Delta a_\mu \leq 41.4 \times 10^{-10}$. The $b \rightarrow s\gamma$ and $(g-2)_\mu$ effects reside at their lower boundaries in the 125 GeV Higgs Strip, as they exert pressure in opposing directions on $M_{1/2}$ since the leading gaugino and squark contributions to $Br(b \rightarrow s\gamma)$ admit an opposite sign to the Standard Model term and Higgs contribution. On the contrary, the effect is additive for the non-Standard Model contribution to Δa_μ , establishing an upper limit on $M_{1/2}$. The SUSY contribution to $Br(b \rightarrow s\gamma)$ cannot be excessively large such that the Standard Model effect becomes minimized, thus necessitating a sufficiently large, or lower bounded, $M_{1/2}$.

The computation of the rare-decay processes for all points in the 125 GeV Higgs Strip are illustrated in Figure (3). We implement a range on the strong coupling constant of $0.1145 \leq \alpha_s(M_Z) \leq 0.1172$ that tightly envelopes the central value of $\alpha_s(M_Z) = 0.1161$ that is supported by recent direct observations [65], introducing a modest uncertainty onto the calculation of each curve in Figure (3), represented by the contour thickness in each pane. All SUSY particle masses, Higgs boson masses, relic densities, and constraints are computed with `MicrOMEGAs 2.4`, applying the proprietary modification of the `SuSpect 2.34` codebase to run the flippon-enhanced RGEs. In Figure (3), the boxed curve segments depict the experimentally observed 2σ values.

We now expand our original Golden Strip to encompass proton decay and dark matter detection experiments. The $p \rightarrow e^+\pi^0$ mode in \mathcal{F} - $SU(5)$ is depicted in Figure (3), indicative of the large pervasive uncertainty propagated into the proton lifetime from the large QCD uncertainties in $\alpha_s(M_Z)$. We apply the Super-Kamiokande established lower bound of 1.4×10^{34} years at the 90% confidence level for the partial lifetime in the $p \rightarrow e^+\pi^0$ mode [66]. For the spin-independent dark matter-nucleon cross section, the XENON100 experiment has probed down to 2×10^{-9} pb (2×10^{-45} cm²) for a WIMP mass of 55 GeV [67], also at the 90% confidence level. The No-Scale \mathcal{F} - $SU(5)$ viable model space shown in Figure (3) lies entirely below this upper bound [8].

Observations of a 130 GeV monochromatic gamma-ray line [68] by the FERMI-LAT Space Telescope have stoked great interest into whether its origin results from dark matter annihilations around the galactic center. The $\chi\chi \rightarrow \gamma\gamma$ line fits a WIMP mass $m_\chi \sim 130$ GeV [68], while a $\chi\chi \rightarrow \gamma Z$ line fits a WIMP mass closer to $m_\chi \sim 145$ GeV [21, 69]. The fit is near $m_\chi \sim 150$ GeV for internal bremsstrahlung [70]. We further allow for the potential combination of all of the above that could land a WIMP mass somewhere in the range $130 \lesssim m_\chi \lesssim 150$ GeV, and as a consequence, we annotate the 130-150 GeV LSP mass region in Figure (3). The most recent FERMI-LAT Collaboration upper bound on the gamma-

ray annihilation cross section is $\langle\sigma v\rangle \sim 10^{-26}$ cm³/s [71], which we use in Figure (3), allowing for a possible subhalo boost factor, which can be on the order of ~ 1000 , as determined from examining extra-galactic clusters [72].

We include in Figure (3) the multi-axis χ^2 of the prior section of this work, computed from those 8 TeV ATLAS multijet searches that display evidence of overproduction above background expectations. The vertical yellow band in Figure (3) depicts the 2σ range around the χ^2 minimum computed from the nominal number of \mathcal{F} - $SU(5)$ simulated events times 0.50, bordered by the lower 2σ boundary at about $M_{1/2} \sim 660$ GeV. The Golden Strip is represented by the cross-hatched region, confined by the lower 2σ boundary on $Br(b \rightarrow s\gamma)$ at its lower $M_{1/2} \sim 545$ GeV limit, and by the lower 2σ boundary on Δa_μ at the Golden Strip's upper $M_{1/2} \sim 760$ GeV limit. Demonstrated in Figure (3) is the intersection of these two bands of model space defined by the 2σ observable regions of completely uncorrelated experiments, though apparently exhibiting interesting evidence of correlated behavior in a No-Scale \mathcal{F} - $SU(5)$ framework. To further heighten the intrigue, the 130-150 GeV LSP model space corresponding to the FERMI-LAT Space Telescope observations of a 130 GeV monochromatic gamma-ray line from the galactic center also very curiously lies snugly within the intersection of all experiments. Notice that the gluino and light stop mass scales are inserted at the bottom of Figure (3). Due to the characteristic rescaling property of No-Scale \mathcal{F} - $SU(5)$, a direct proportional relationship exists between the SUSY spectrum and gaugino $M_{1/2}$, permitting a simple visual inspection of the associated gluino and light stop masses for any specified $M_{1/2}$.

It is worth emphasizing again that all points delineated by the curves in each pane in Figure (3) are themselves the intersection of three critical parameters measured to high precision in current experiments, namely the 7-year WMAP relic density $0.1088 \leq \Omega h^2 \leq 0.1158$, a 124-127 GeV light Higgs boson mass, and a $172.2 \leq m_t \leq 174.4$ GeV top quark mass. Therefore, at the present time, we can find no experiment pertinent to the supersymmetric parameter space that is not in conformance with the narrow band of No-Scale \mathcal{F} - $SU(5)$ model space from $660 \lesssim M_{1/2} \lesssim 760$ GeV, which corresponds to sparticle masses of $133 \lesssim M(\tilde{\chi}_1^0) \lesssim 160$ GeV, $725 \lesssim M(\tilde{t}_1) \lesssim 845$ GeV, and $890 \lesssim M(\tilde{g}) \lesssim 1025$ GeV. Such a mutual interrelation between all relevant experiments seems to strongly belie attribution to random stochastics.

The proximity of the 145-150 GeV LSP strip that resides within the theoretically and phenomenologically favored \mathcal{F} - $SU(5)$ parameter space defined by all model constraints, in relation to the minimum of our multi-axis χ^2 curve, recalls to mind a very similar level of statistical adjacency shared by the updated χ^2 curves for the experimental Higgs boson mass measurements ($m_h \sim 125$ GeV) with the mass region theoretically and phenomenologically favored by electroweak precision measurements at $m_h = 94_{-24}^{+29}$ GeV [73]. The difference of about one stan-

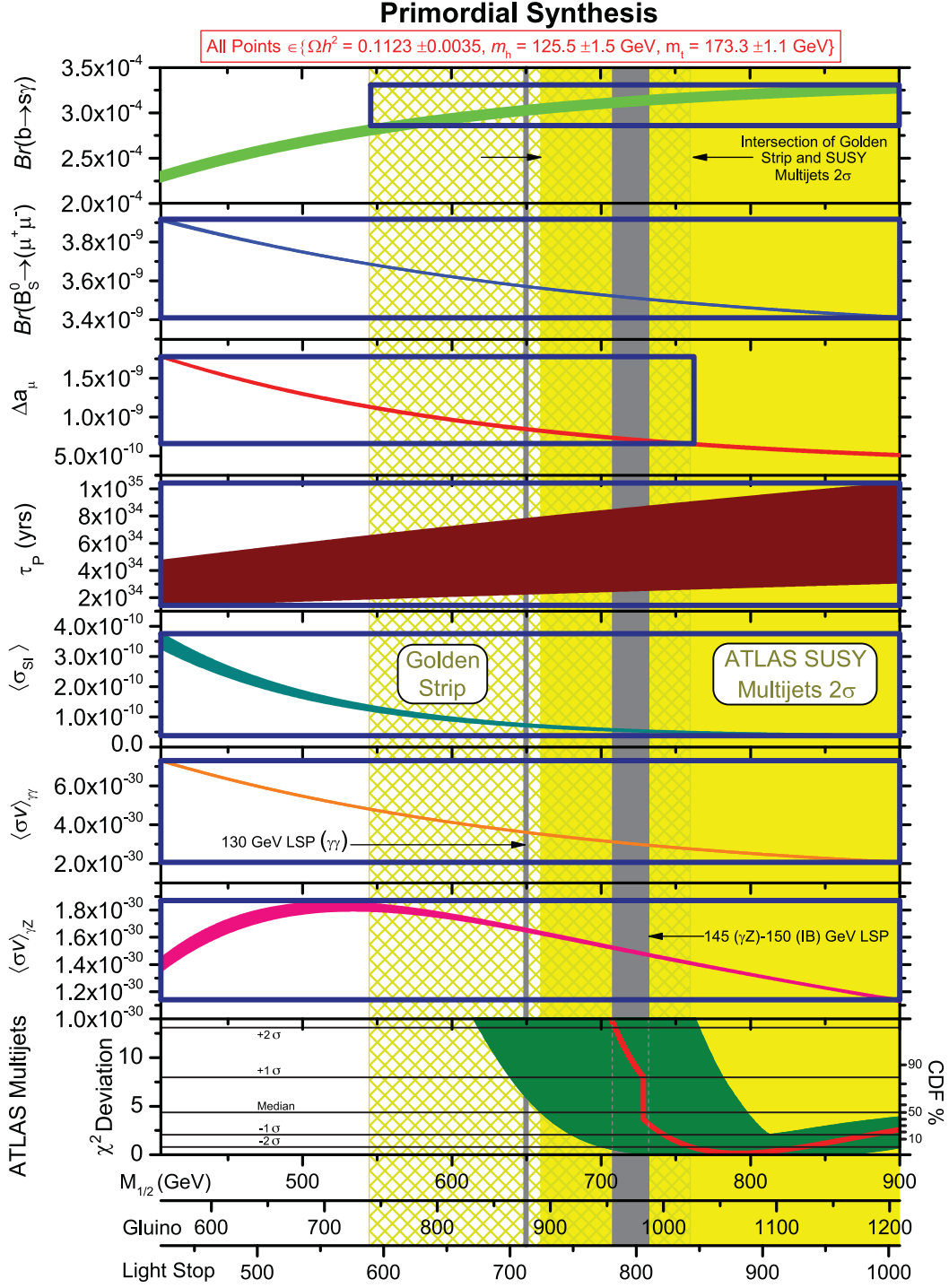


FIG. 3: Primordial Synthesis of all currently progressing experiments searching for physics beyond the Standard Model. All points depicted on each curve satisfy the conditions $0.1088 \leq \Omega h^2 \leq 0.1158$, $124 \leq m_h \leq 127$ GeV, and $172.2 \leq m_t \leq 174.4$ GeV. Each curve thickness represents an uncertainty on the strong coupling constant $0.1145 \leq \alpha_s(M_Z) \leq 0.1172$ (excluding the χ^2 pane). The multi-axis χ^2 deviation in the bottom pane comprises an uncertainty derived from an increase and decrease by a factor of 2 around the χ^2 computed on the nominal number of \mathcal{F} - $SU(5)$ events surviving all cuts (nominal value shown in center of shaded curve). The cross-hatched region illustrates the Golden Strip, which identifies the intersection of all current BSM experiments, excluding the ATLAS collider studies. The yellow region portrays the 2σ uncertainty on the χ^2 computed from \mathcal{F} - $SU(5)$ Events $\times 0.5$. We highlight the 130 GeV and 145-150 GeV LSP masses by the vertical strips. Notice that we have inserted the gluino and light stop mass scales at the bottom of the Figure to enable an instant conversion from the gaugino mass $M_{1/2}$, made possible by the characteristic rescaling property of the \mathcal{F} - $SU(5)$ SUSY spectrum in terms of $M_{1/2}$.

standard deviation between the empirically measured Higgs boson mass and the electroweak precision favored region is roughly akin to the statistical margin separating the LHC SUSY multijet measurements and the optimum phenomenological \mathcal{F} - $SU(5)$ region, where we would assign, based upon the Figure (2) analysis, a standard fluctuation width of about 60 GeV to deviations in the downward mass direction, and 200 GeV to the upper χ^2 median intersection. Thus, we may take great satisfaction that such a level of consistency is displayed between experiment and theory in \mathcal{F} - $SU(5)$, supported by relevant historical precedent.

As two points of potentially relevant interest, we must also remark in passing on recent developments regarding the measurement of the top quark mass and the strong coupling constant. An external study based on ATLAS inclusive jet cross section data [74] has suggested the value $\alpha_s(M_Z) = 0.1151$, which is slightly lower than the world central value of 0.1161 on which we above remarked. Also, the CMS Collaboration has recently announced [75] the world's single most precise top quark mass measurement at $m_h = 173.49 \pm 1.07$ GeV, with a central value slightly above the existing world average. Moreover, the latest measurements by ATLAS show central values of $m_t = 174.5$ GeV [76], $m_t = 174.9$ GeV [77], and $m_t = 175.2$ GeV [78], all modestly elevated above the world average central value. In Ref. [21], we investigated on the roles that a slightly elevated top quark mass, and a slightly reduced strong coupling could play in facilitating satisfaction of the central Higgs mass measurements in the range of 125–126 GeV, without resorting to an overly heavy squark spectrum or extremities in the error margins for the Higgs mass itself. The lowering of α_s while maintaining consistency with precision electroweak scale data is an accommodation to which the flipped $SU(5)$ GUT is particularly well historically adapted [79]. An interesting side effect of this modification is an escalation in the proton decay rate linked to a parallel reduction in the GUT scale M_{32} .

We close our discussion of Figure (3) by remarking on the striking familiarity of this figure to the correlation of predicted and observed light elemental abundances with the value of the baryon-to-photon ratio given by the observations of the Cosmic Microwave Background (CMB) by WMAP. The amazing consistency with which predictions of light element abundances by Primordial Nucleosynthesis demonstrates with astronomical observations, while also compatible with the independently measured CMB, provide powerful corroboration of the Big Bang Theory. We envision a compelling parallel here amongst the synthesis of light elements predicted by Primordial Nucleosynthesis and observed by experiments, with the synthesis in an ubiquitous \mathcal{F} - $SU(5)$ structure

in nature of all currently progressing experiments searching for physics beyond the Standard Model, to which we aptly offer the description *Primordial Synthesis*. Analogous to the consistency encountered between theory and experiment of light elemental abundances in Primordial Nucleosynthesis that provides a convincing connection to the Big Bang Theory, we suggest that the consistency revealed in Figure (3) between all the BSM experiments in No-Scale \mathcal{F} - $SU(5)$ Primordial Synthesis presents persuasive indications of BSM physics currently being probed at the LHC and indeed possibly all the experiments involved in searching for the parameters in Figure (3).

VI. CONCLUSIONS

We evaluated the first $\sqrt{s} = 8$ TeV 5.8 fb^{-1} ATLAS SUSY multijet data observations within the context of No-Scale \mathcal{F} - $SU(5)$ and suggested a simple mechanism for improving the efficiency of capture for SUSY multijet events. The \mathcal{F} - $SU(5)$ best SUSY mass spectrum fit to the 8 TeV data was found to be consistent with our 7 TeV results, within a prescribed 2σ margin of error. These findings were synthesized with the complete amalgamation of experiments currently searching for beyond the Standard Model physics, discovering hidden correlations suggestive of deeper fundamental underpinnings. The Primordial Synthesis of all BSM experiments uncovers a highly favorable region of the \mathcal{F} - $SU(5)$ model space spanning from $660 \lesssim M_{1/2} \lesssim 760$ GeV, corresponding to sparticle masses of $133 \lesssim M(\tilde{\chi}_1^0) \lesssim 160$ GeV, $725 \lesssim M(\tilde{t}_1) \lesssim 845$ GeV, and $890 \lesssim M(\tilde{g}) \lesssim 1025$ GeV. We project that if indeed the production of events beyond the Standard Model expectations in those active SUSY multijet searches studied here can be attributed to new physics, then the completion of the 8 TeV run at the LHC in 2012 could provide a strong indication of new physics.

Acknowledgments

We thank Tommaso Dorigo for helpful discussions on the LHC supersymmetry search. This research was supported in part by the DOE grant DE-FG03-95-Er-40917 (TL and DVN), by the Natural Science Foundation of China under grant numbers 10821504, 11075194, 11135003, and 11275246 (TL), and by the Mitchell-Heep Chair in High Energy Physics (JAM). We also thank Sam Houston State University for providing high performance computing resources.

[1] T. Li, J. A. Maxin, D. V. Nanopoulos, and J. W. Walker, "The Golden Point of No-Scale and No-Parameter \mathcal{F} -

$SU(5)$," Phys. Rev. **D83**, 056015 (2011), 1007.5100.

- [2] T. Li, J. A. Maxin, D. V. Nanopoulos, and J. W. Walker, “The Golden Strip of Correlated Top Quark, Gaugino, and Vectorlike Mass In No-Scale, No-Parameter F-SU(5),” *Phys. Lett.* **B699**, 164 (2011), 1009.2981.
- [3] T. Li, J. A. Maxin, D. V. Nanopoulos, and J. W. Walker, “Super No-Scale \mathcal{F} -SU(5): Resolving the Gauge Hierarchy Problem by Dynamic Determination of $M_{1/2}$ and $\tan\beta$,” *Phys. Lett. B* **703**, 469 (2011), 1010.4550.
- [4] T. Li, J. A. Maxin, D. V. Nanopoulos, and J. W. Walker, “Blueprints of the No-Scale Multiverse at the LHC,” *Phys. Rev.* **D84**, 056016 (2011), 1101.2197.
- [5] T. Li, J. A. Maxin, D. V. Nanopoulos, and J. W. Walker, “Ultra High Jet Signals from Stringy No-Scale Supergravity,” (2011), 1103.2362.
- [6] T. Li, J. A. Maxin, D. V. Nanopoulos, and J. W. Walker, “The Ultrahigh jet multiplicity signal of stringy no-scale \mathcal{F} -SU(5) at the $\sqrt{s} = 7$ TeV LHC,” *Phys.Rev.* **D84**, 076003 (2011), 1103.4160.
- [7] T. Li, J. A. Maxin, D. V. Nanopoulos, and J. W. Walker, “The Unification of Dynamical Determination and Bare Minimal Phenomenological Constraints in No-Scale F-SU(5),” *Phys.Rev.* **D85**, 056007 (2012), 1105.3988.
- [8] T. Li, J. A. Maxin, D. V. Nanopoulos, and J. W. Walker, “The Race for Supersymmetric Dark Matter at XENON100 and the LHC: Stringy Correlations from No-Scale F-SU(5),” (2011), 1106.1165.
- [9] T. Li, J. A. Maxin, D. V. Nanopoulos, and J. W. Walker, “A Two-Tiered Correlation of Dark Matter with Missing Transverse Energy: Reconstructing the Lightest Supersymmetric Particle Mass at the LHC,” *JHEP* **02**, 129 (2012), 1107.2375.
- [10] T. Li, J. A. Maxin, D. V. Nanopoulos, and J. W. Walker, “Prospects for Discovery of Supersymmetric No-Scale F-SU(5) at The Once and Future LHC,” *Nucl.Phys.* **B859**, 96 (2012), 1107.3825.
- [11] T. Li, J. A. Maxin, D. V. Nanopoulos, and J. W. Walker, “Has SUSY Gone Undetected in 9-jet Events? A Ten-Fold Enhancement in the LHC Signal Efficiency,” (2011), 1108.5169.
- [12] T. Li, J. A. Maxin, D. V. Nanopoulos, and J. W. Walker, “Natural Predictions for the Higgs Boson Mass and Supersymmetric Contributions to Rare Processes,” *Phys.Lett.* **B708**, 93 (2012), 1109.2110.
- [13] T. Li, J. A. Maxin, D. V. Nanopoulos, and J. W. Walker, “The F-Landscape: Dynamically Determining the Multiverse,” *Inter.Jour.Mod.Phys.* **A27**, 1250121 (2012), 1111.0236.
- [14] T. Li, J. A. Maxin, D. V. Nanopoulos, and J. W. Walker, “Profumo di SUSY: Suggestive Correlations in the ATLAS and CMS High Jet Multiplicity Data,” (2011), 1111.4204.
- [15] T. Li, J. A. Maxin, D. V. Nanopoulos, and J. W. Walker, “A Higgs Mass Shift to 125 GeV and A Multi-Jet Supersymmetry Signal: Miracle of the Flippons at the $\sqrt{s} = 7$ TeV LHC,” *Phys.Lett.* **B710**, 207 (2012), 1112.3024.
- [16] T. Li, J. A. Maxin, D. V. Nanopoulos, and J. W. Walker, “A Multi-Axis Best Fit to the Collider Supersymmetry Search: The Aroma of Stops and Gluinos at the $\sqrt{s} = 7$ TeV LHC,” (2012), 1203.1918.
- [17] T. Li, J. A. Maxin, D. V. Nanopoulos, and J. W. Walker, “Chanel $N^{\circ}5(\text{fb}^{-1})$: The Sweet Fragrance of SUSY,” (2012), 1205.3052.
- [18] T. Li, J. A. Maxin, D. V. Nanopoulos, and J. W. Walker, “Non-trivial Supersymmetry Correlations between ATLAS and CMS Observations,” (2012), 1206.0293.
- [19] T. Li, J. A. Maxin, D. V. Nanopoulos, and J. W. Walker, “Correlating LHCb $B_s^0 \rightarrow \mu^+\mu^-$ Results with the ATLAS-CMS Multijet Supersymmetry Search,” *Europhysics.Lett.* **In Press** (2012), 1206.2633.
- [20] T. Li, J. A. Maxin, D. V. Nanopoulos, and J. W. Walker, “Testing No-Scale \mathcal{F} -SU(5): A 125 GeV Higgs Boson and SUSY at the 8 TeV LHC,” *Phys.Lett.* **B In Press** (2012), 1207.1051.
- [21] T. Li, J. A. Maxin, D. V. Nanopoulos, and J. W. Walker, “A 125.5 GeV Higgs Boson in \mathcal{F} -SU(5): Imminently Observable Proton Decay, A 130 GeV Gamma-ray Line, and SUSY Multijets & Light Stops at the LHC,” (2012), 1208.1999.
- [22] “Search for new phenomena using large jet multiplicities and missing transverse momentum with ATLAS in 5.8 fb^{-1} of $\sqrt{s} = 8$ TeV proton-proton collisions,” (2012), ATLAS-CONF-2012-103, URL <http://cdsweb.cern.ch>.
- [23] “Search for squarks and gluinos with the ATLAS detector using final states with jets and missing transverse momentum at $\sqrt{s} = 8$ TeV,” (2012), ATLAS-CONF-2012-109, URL <http://cdsweb.cern.ch>.
- [24] “Search for squarks and gluinos with the ATLAS detector using final states with jets and missing transverse momentum and 4.7 fb^{-1} of $\sqrt{s} = 7$ TeV proton-proton collision data,” (2012), ATLAS-CONF-2012-033, 1208.0949, URL <http://cdsweb.cern.ch>.
- [25] G. Aad et al. (ATLAS Collaboration), “Hunt for new phenomena using large jet multiplicities and missing transverse momentum with ATLAS in 4.7 fb^{-1} of $\sqrt{s} = 7$ TeV proton-proton collisions,” *JHEP* **1207**, 167 (2012), 1206.1760.
- [26] S. Badger, B. Biedermann, P. Uwer, and V. Yundin, “NLO QCD corrections to multi-jet production at the LHC with a centre-of-mass energy of $\sqrt{s} = 8$ TeV,” (2012), 1209.0098.
- [27] B. Nachman and T. Rudelius, “Evidence for Excessive Conservatism in LHC SUSY Searches,” (2012), 1209.3522.
- [28] E. Cremmer, S. Ferrara, C. Kounnas, and D. V. Nanopoulos, “Naturally Vanishing Cosmological Constant in $N = 1$ Supergravity,” *Phys. Lett.* **B133**, 61 (1983).
- [29] J. R. Ellis, C. Kounnas, and D. V. Nanopoulos, “No Scale Supersymmetric Guts,” *Nucl. Phys.* **B247**, 373 (1984).
- [30] S. Ferrara, C. Kounnas, and F. Zwirner, “Mass formulae and natural hierarchy in string effective supergravities,” *Nucl. Phys.* **B429**, 589 (1994), hep-th/9405188.
- [31] E. Witten, “Dimensional Reduction of Superstring Models,” *Phys. Lett.* **B155**, 151 (1985).
- [32] T.-j. Li, J. L. Lopez, and D. V. Nanopoulos, “Compactifications of M theory and their phenomenological consequences,” *Phys.Rev.* **D56**, 2602 (1997), hep-ph/9704247.
- [33] D. V. Nanopoulos, “F-enomenology,” (2002), hep-ph/0211128.
- [34] S. M. Barr, “A New Symmetry Breaking Pattern for $SO(10)$ and Proton Decay,” *Phys. Lett.* **B112**, 219 (1982).
- [35] J. P. Derendinger, J. E. Kim, and D. V. Nanopoulos, “Anti-SU(5),” *Phys. Lett.* **B139**, 170 (1984).
- [36] I. Antoniadis, J. R. Ellis, J. S. Hagelin, and D. V. Nanopoulos, “Supersymmetric Flipped SU(5) Revitalized,” *Phys. Lett.* **B194**, 231 (1987).
- [37] J. Jiang, T. Li, and D. V. Nanopoulos, “Testable Flipped

- $SU(5) \times U(1)_X$ Models,” Nucl. Phys. **B772**, 49 (2007), hep-ph/0610054.
- [38] J. L. Lopez, D. V. Nanopoulos, and K.-j. Yuan, “The Search for a realistic flipped $SU(5)$ string model,” Nucl. Phys. **B399**, 654 (1993), hep-th/9203025.
- [39] J. Jiang, T. Li, D. V. Nanopoulos, and D. Xie, “ F - $SU(5)$,” Phys. Lett. **B677**, 322 (2009).
- [40] O. Buchmueller, R. Cavanaugh, M. Citron, A. De Roeck, M. Dolan, J. Ellis, et al., “The CMSSM and NUHM1 in Light of 7 TeV LHC, $B_s \rightarrow \mu^+ \mu^-$ and XENON100 Data,” (2012), 1207.7315.
- [41] “Search for supersymmetry in all-hadronic events with α_T ,” (2011), CMS PAS SUS-11-003, URL <http://cdsweb.cern.ch>.
- [42] G. Aad et al. (Atlas Collaboration), “Search for new phenomena in final states with large jet multiplicities and missing transverse momentum using $\sqrt{s} = 7$ TeV pp collisions with the ATLAS detector,” JHEP **1111**, 099 (2011), 1110.2299.
- [43] G. Aad et al. (ATLAS Collaboration), “Search for squarks and gluinos using final states with jets and missing transverse momentum with the ATLAS detector in $\sqrt{s} = 7$ TeV proton-proton collisions,” (2011), 1109.6572.
- [44] “Search for direct top squark pair production in final states with one isolated lepton, jets, and missing transverse momentum in $\sqrt{s} = 7$ TeV pp collisions using 4.7 fb $^{-1}$ of ATLAS data,” (2012), ATLAS-CONF-2012-073, URL <http://cdsweb.cern.ch>.
- [45] J. Conway et al., “PGS4: Pretty Good (Detector) Simulation,” (2009), URL <http://www.physics.ucdavis.edu/~conway/research/>.
- [46] T. Stelzer and W. F. Long, “Automatic generation of tree level helicity amplitudes,” Comput. Phys. Commun. **81**, 357 (1994), hep-ph/9401258.
- [47] J. Alwall et al., “MadGraph/MadEvent Collider Event Simulation Suite,” (2011), URL <http://madgraph.hep.uiuc.edu/>.
- [48] J. Alwall et al., “MadGraph/MadEvent v4: The New Web Generation,” JHEP **09**, 028 (2007), 0706.2334.
- [49] T. Sjostrand, S. Mrenna, and P. Z. Skands, “PYTHIA 6.4 Physics and Manual,” JHEP **05**, 026 (2006), hep-ph/0603175.
- [50] G. Belanger, F. Boudjema, P. Brun, A. Pukhov, S. Rosier-Lees, et al., “Indirect search for dark matter with micrOMEGAs2.4,” Comput.Phys.Commun. **182**, 842 (2011), 1004.1092.
- [51] A. Djouadi, J.-L. Kneur, and G. Moultaka, “SuSpect: A Fortran code for the supersymmetric and Higgs particle spectrum in the MSSM,” Comput. Phys. Commun. **176**, 426 (2007), hep-ph/0211331.
- [52] J. W. Walker, “CutLHCO: A Consumer-Level Tool for Implementing Generic Collider Data Selection Cuts in the Search for New Physics,” (2012), 1207.3383.
- [53] T. Aoyama, M. Hayakawa, T. Kinoshita, and M. Nio, “Complete Tenth-Order QED Contribution to the Muon $g-2$,” (2012), 1205.5370.
- [54] “Combination of CDF and D0 Results on the Mass of the Top Quark using up to 5.6 fb $^{-1}$ of data (The CDF and D0 Collaboration),” (2010), 1007.3178.
- [55] E. Komatsu et al. (WMAP), “Seven-Year Wilkinson Microwave Anisotropy Probe (WMAP) Observations: Cosmological Interpretation,” Astrophys.J.Suppl. **192**, 18 (2010), 1001.4538.
- [56] G. Aad et al. (ATLAS Collaboration), “Observation of a new particle in the search for the Standard Model Higgs boson with the ATLAS detector at the LHC,” Phys.Lett. **B716**, 1 (2012), 1207.7214.
- [57] S. Chatrchyan et al. (CMS Collaboration), “Observation of a new boson at a mass of 125 GeV with the CMS experiment at the LHC,” Phys.Lett. **B716**, 30 (2012), 1207.7235.
- [58] T. Aaltonen et al. (CDF Collaboration, D0 Collaboration), “Evidence for a particle produced in association with weak bosons and decaying to a bottom-antibottom quark pair in Higgs boson searches at the Tevatron,” Phys.Rev.Lett. **109**, 071804 (2012), 1207.6436.
- [59] E. Barberio et al. (Heavy Flavor Averaging Group (HFAG)), “Averages of b -hadron properties at the end of 2006,” (2007), 0704.3575.
- [60] M. Artuso, E. Barberio, and S. Stone, “ B Meson Decays,” PMC Phys. **A3**, 3 (2009), 0902.3743.
- [61] M. Misiak, “QCD challenges in radiative B decays,” AIP Conf.Proc. **1317**, 276 (2011), 1010.4896.
- [62] M. Misiak et al., “The first estimate of $\text{Br}(\overline{B} \rightarrow X_s \gamma)$ at $\mathcal{O}(\alpha_s^2)$,” Phys. Rev. Lett. **98**, 022002 (2007), hep-ph/0609232.
- [63] T. Becher and M. Neubert, “Analysis of $\text{Br}(\overline{B} \rightarrow X_s \gamma)$ at NNLO with a cut on photon energy,” Phys. Rev. Lett. **98**, 022003 (2007), hep-ph/0610067.
- [64] R. Aaij et al. (LHCb collaboration), “Strong constraints on the rare decays $B_s \rightarrow \mu^+ \mu^-$ and $B^0 \rightarrow \mu^+ \mu^-$,” Phys.Rev.Lett. **108**, 231801 (2012), 1203.4493.
- [65] D. Bandurin (D0 and CDF Collaborations), “QCD measurements at the Tevatron,” (2011), 1112.0051.
- [66] J. Hewett, H. Weerts, R. Brock, J. Butler, B. Casey, et al., “Fundamental Physics at the Intensity Frontier,” (2012), 1205.2671.
- [67] E. Aprile et al. (XENON100 Collaboration), “Dark Matter Results from 225 Live Days of XENON100 Data,” (2012), 1207.5988.
- [68] C. Weniger, “A Tentative Gamma-Ray Line from Dark Matter Annihilation at the Fermi Large Area Telescope,” (2012), 1204.2797.
- [69] M. Su and D. P. Finkbeiner, “Strong Evidence for Gamma-ray Line Emission from the Inner Galaxy,” (2012), 1206.1616.
- [70] T. Bringmann, X. Huang, A. Ibarra, S. Vogl, and C. Weniger, “Fermi LAT Search for Internal Bremsstrahlung Signatures from Dark Matter Annihilation,” (2012), 1203.1312.
- [71] M. Ackermann et al. (LAT Collaboration), “Fermi LAT Search for Dark Matter in Gamma-ray Lines and the Inclusive Photon Spectrum,” Phys.Rev. **D86**, 022002 (2012), 1205.2739.
- [72] A. Hektor, M. Raidal, and E. Tempel, “An evidence for indirect detection of dark matter from galaxy clusters in Fermi-LAT data,” (2012), 1207.4466.
- [73] L. E. W. Group (2012), Blue Band Higgs χ^2 plot, URL <http://lepewwg.web.cern.ch/LEPEWWG/>.
- [74] B. Malaescu, “Evaluation of α_s using the ATLAS inclusive jet cross-section data,” (2012), 1210.1383.
- [75] S. Chatrchyan et al. (The CMS Collaboration), “Measurement of the top-quark mass in $t\bar{t}$ events with lepton+jets final states in pp collisions at $\sqrt{s} = 7$ TeV,” (2012), 1209.2319.
- [76] G. Aad et al. (ATLAS Collaboration), “Measurement of the top quark mass with the template method in the $t\bar{t} \rightarrow$ lepton + jets channel using ATLAS data,” Eur.Phys.J.

- C72**, 2046 (2012), 1203.5755.
- [77] “Determination of the Top Quark Mass with a Template Method in the All-Hadronic Decay Channel using 2.04 fb⁻¹ of ATLAS Data,” (2012), ATLAS-CONF-2012-030, URL <http://cdsweb.cern.ch>.
- [78] “Top-quark mass measurement in the $e\mu$ channel using the m_{T2} variable at ATLAS,” (2012), ATLAS-CONF-2012-082, URL <http://cdsweb.cern.ch>.
- [79] J. R. Ellis, J. L. Lopez, and D. V. Nanopoulos, “Lowering α_s by flipping SU(5),” Phys.Lett. **B371**, 65 (1996), hep-ph/9510246.